diversity

MDPI

Article

Study on the Diversity of Flower Color Phenotypes in *Paeonia delavayi*

Siqi Liu [1], Huiyao Li [1], Juan Wang [1,*], Chun Du [1], Yue Pan [1], Guiqing He [2,3], Jianying Xiang [1] and Jin Li [4]

[1] College of Forestry, Southwest Forestry University, Kunming 650224, China; cc_77@swfu.edu.cn (S.L.); lhy@swfu.edu.cn (H.L.); 18724906907@163.com (C.D.); panyue96@163.com (Y.P.)
[2] College of Landscape and Horticulture, Southwest Forestry University, Kunming 650224, China
[3] Institute of Alpine Economic Plants, Yunnan Academy of Agricultural Sciences, Lijiang 674100, China
[4] Institute of Forestry Industry, Yunnan Academy of Forestry and Grassland, Kunming 650224, China
* Correspondence: schima@swfu.edu.cn

Abstract

Paeonia delavayi displays exceptionally diverse flower colors. This study established a quantitative classification system for these colors and analyzed the relationships among pigment composition, content, and geographical distribution, providing a scientific basis for genetic diversity conservation and ornamental peony breeding. Petals from 465 plants across 30 wild populations and nurseries in central and northwestern Yunnan, China, were analyzed. Color values were quantified using CIE-Lab and Munsell color systems, while pigment content was determined using HPLC and spectrophotometry. Correlations between color values, pigments, and environmental factors were examined. The results were as follows: (1) Flower colors were classified into nine color series, each with distinct boundaries in the color value space: white (W), yellow (Y), yellow-green (YG), orange (O), orange-brown (OB), pink (P), red (R), purple-red (PR), and dark purple (DP). (2) Color values showed wide variation (a^*: −23.10–65.54; b^*: −4.11–94.26), indicating high diversity. (3) Yellow-category petals had high b^* values (24.91–94.26), correlated with carotenoid, chlorophyll, and flavonoid content, and lacked anthocyanins. The lightness value (L^*) of red-category petals was correlated with total flavonoid (TF) and total anthocyanin (ACN) content. (4) Correlation analysis showed that the formation of dark-flower colors (DP, PR, R) was significantly and positively correlated with high altitude, high soil organic carbon (SOC), and high soil total nitrogen (STN) content. The distribution of yellow-series flower colors (Y, YG) was correlated with lower altitude and weaker UV radiation, while increasing mean annual temperature (MAT) limited their distribution. (5) Analysis incorporating environmental factors showed that high-altitude areas in northwestern Yunnan, such as Shangri-La and Lijiang, had the richest flower color diversity, whereas central Yunnan's low-altitude areas were dominated by yellow flower colors. This study indicates that the high-altitude areas of northwestern Yunnan represent the region with the richest flower color diversity in *P. delavayi*, and are important for the conservation of its flower color genetic diversity and as a source of genetic diversity in flower color in ornamental cultivar breeding.

Keywords: *Paeonia delavayi*; flower color classification; CIE-Lab color system; Munsell color system; pigments; geographical distribution

Check for updates

Academic Editor: Mario A. Pagnotta

Received: 27 January 2026
Revised: 27 February 2026
Accepted: 27 February 2026
Published: 8 March 2026

Copyright: © 2026 by the authors. Licensee MDPI, Basel, Switzerland. This article is an open access article distributed under the terms and conditions of the Creative Commons Attribution (CC BY) license.

1. Introduction

As one of the basal groups of the angiosperm phylogenetic tree, *Paeonia* plants are invaluable and important for studying the phylogenetic evolution of angiosperms as well as

for conserving germplasm [1]. Nine plant species from *Paeonia* (Paeoniaceae) sect. *Moutan* DC. are listed in the *Flora of China* (2001). These species are all designated as national key protected wild plants species and are indigenous to China [2]. *Paeonia delavayi* is the southernmost and most extensively distributed species in the *Paeonia* group. It occurs at altitudes ranging from 1850 m to 4000 m in central and northwestern Yunnan, southwestern Sichuan, and southeastern Tibet, between latitudes 24° N and 32° N and longitudes 94° E and 104° E. This species is adapted to a range of climates, from mid-subtropical to Qinghai–Tibet alpine [3,4]. The germplasm of *P. delavayi* is characterized by an exceptional variety of flower colors, including white, green, yellow, pink, red, and dark purple, as well as by a distinctive yellow-petal-related genetic locus. It serves as a major parental source for current yellow peony cultivars with substantial ornamental value, such as High Noon, Alice Harding, and the Itoh hybrid series [5–7]. These features highlight its importance in *Paeonia* section germplasm research and genetic diversity preservation, along with its considerable potential for the development of new varieties.

Current research on the genetic diversity of *P. delavayi* involves aspects such as phenotypic characteristics [8], physicochemical properties [9,10], molecular marker analysis [11,12], and genetic differentiation [13]. In studies of phenotypic diversity, qualitative descriptions and analyses of the diverse flower colors of *P. delavayi* have been limited to visual inspection or comparison with the Royal Horticultural Society Colour Chart (RHSCC). Based on these methods, the flower colors of *P. delavayi* have been classified into categories such as yellow, light yellow, orange-yellow, orange, yellow-green, green, red, purple-red, purple, dark purple, pink, and dark red, etc. [14,15]. Colors are determined by human visual assessment under the RHSCC color chart system, which uses numerical and alphabetical codes in place of natural color names or quantitative colorimetric criteria. The development of a single, objective, and measurable standard for flower color identification is hampered by this method's high sensitivity to subjective factors and ambient light conditions [16]. The internationally standardized color language, the CIE-Lab color system, which is accurately represented by the values of L^* (lightness), a^* (redness/greenness), and b^* (yellowness/blueness), has been extensively used for quantitative analysis of flower colors [17]. Moreover, the Munsell color system was the earliest framework to quantitatively describe the human perception of color [18]. It facilitates the identification of specific color names within the ISCC-NBS Color Name Chart according to Hue (H), Value (V), and Saturation (S), so augmenting the CIE-Lab color system [19]. The color values of the two color-series systems are mutually convertible [20], and their combined application can furnish objective, quantifiable and repeatable color values (L^*, a^*, b^*; H, V, C), thereby mitigating or eliminating inconsistencies arising from the observational environment and inter-individual variation. It is effective for quantitative analysis of flower color and color system categorization studies of plants with distinct floral colors, such as *Rosa* [21], *Hemerocallis* [22], and *Chrysanthemum* [23]. Multiple varieties of *Gerbera hybrida* exhibit distinct flower colors, including white, yellow, orange, pink, red, and purple [24]. Reports have also applied this method for the quantitative classification of the flower color phenotype of *P. rockii*, categorizing it into six color series (white, pink, red, purplish red, dark red, and bicolor) [25], while also classifying *P. suffruticosa* into eight-color series (pink, white, red, green, gray, blue, purple, and black) [26].

Paeonia delavayi has consistently been a species of interest because to the diversity and distinctiveness of its floral color phenotype. The Chinese Virtual Herbarium (CVH) catalogs 543 specimens (after removal of duplicates) collected from 47 counties and cities across the provinces of Yunnan, Sichuan, and Tibet between 1908 and 2014, within a geographic range of 24°48′ to 32°56′ N and 93°41′ to 108°12′ E, at altitudes ranging from 2000 m to 3800 m. The specimen data gathered throughout this extensive area only documents yellow

and red for the petals, and it is noteworthy that color identification is no longer available in herbarium specimens. Therefore, these data inadequately represent the extent of color diversity within the yellow and red color series of the *P. delavayi* petal germplasm. This study seeks to examine the variation and diversity characteristics of *P. delavayi* petal color by sampling over 30 wild populations and germplasm nurseries in Yunnan Province, the primary distribution area of *P. delavayi*.

This study focuses on the flower color diversity of *P. delavayi*, with the following research goals: (1) to establish a quantitative classification system for its petal color based on the CIE-Lab and Munsell color systems through cluster analysis; (2) to investigate the composition and content of core pigments (total flavonoids, anthocyanins, carotenoids, chlorophyll) in petals of different color phenotypes; (3) to analyze the intrinsic connections among flower color values, pigment properties, and geographical environmental factors; and (4) to lay a scientific foundation for the conservation of *P. delavayi* genetic diversity and the breeding of ornamental peonies.

2. Materials and Methods

2.1. Experimental Material

Based on relevant literature and the preliminary field survey data of our research group, sampling sites were selected to cover the main distribution areas of *P. delavayi* in Yunnan Province, China, while ensuring the representation of all observed flower color morphs across the region. Prior to formal sampling, we systematically sorted the preliminarily surveyed population sites by latitude (ranging from 25°01′32″ N to 28°27′24.67″ N) to establish a latitudinal gradient-based sampling framework, which aimed to capture the geographic variation of the species across its distribution range in Yunnan. Between April 2020 and May 2024, field investigations were conducted using a stratified random sampling method integrated with latitudinal stratification. A total of 30 wild populations and three germplasm nurseries were sampled, spanning key regions including Kunming, Lijiang, and Dêqên Tibetan Autonomous Prefecture (Table 1). The sampling framework adopted a two-level stratification: (1) primary strata were defined by latitudinal zones to account for broad geographic gradients; and (2) secondary strata within each population were classified by flower color morphs to ensure proportional representation of all color types.

Table 1. Compilation of 30 wild populations and 3 germplasm nurseries of *P. delavayi* along with their corresponding acronyms.

No.	Sampling Sites of Yunnan, China	Abbreviation	Longitude	Latitude	Altitude, m.a.s.l.	Number of Specimens
0	Mingyong Glacier, Yunling Township, Dêqên County, Dêqên Tibetan Autonomous Prefecture	MY	98°45′59″ E	28°27′25″ N	2890	13
1	Yeri Village, Nixi Township, Shangri-La City, Dêqên Tibetan Autonomous Prefecture	YRC	99°8′22″ E	28°24′4″ N	2700	1
2	No. 7 Bridge, Baima Snow Mountain, Dêqên County, Dêqên Tibetan Autonomous Prefecture	BM7	99°11′2″ E	28°17′14″ N	3231	5
3	Shusong Village, Benzilan Town, Dêqên County, Dêqên Tibetan Autonomous Prefecture	SSC	99°11′5″ E	28°16′32″ N	2836	3
4	Xinyang Village, Nixi Township, Shangri-La City, Dêqên Tibetan Autonomous Prefecture	XYC	99°28′37″ E	28°3′54″ N	3249	11

Table 1. *Cont.*

No.	Sampling Sites of Yunnan, China	Abbreviation	Longitude	Latitude	Altitude, m.a.s.l.	Number of Specimens
5	Gêza Township, Shangri-La City, Dêqên Tibetan Autonomous Prefecture	GZ	99°47′2″ E	28°0′27″ N	3186	9
6	Tangdui Village, Nixi Township, Shangri-La City, Dêqên Tibetan Autonomous Prefecture	GHT	99°32′19″ E	27°59′36″ N	2844	7
7	Ski Resort, Shangri-La City, Dêqên Tibetan Autonomous Prefecture	HXC	99°35′22″ E	27°56′48″ N	3420	97
8	Botanical Garden, Shangri-La City, Dêqên Tibetan Autonomous Prefecture	ZWY	99°38′19″ E	27°54′18″ N	3356	11
9	Caopidian, Yongning Township, Ninglang County, Lijiang City	CPD	100°28′23″ E	27°45′4″ N	2860	4
10	Lazi, Labo Township, Ninglang County, Lijiang City	LZ	100°29′59″ E	27°44′44″ N	2801	7
11	Lazi Reservoir, Labo Township, Ninglang County, Lijiang City	LZSK	100°30′55″ E	27°44′39″ N	2769	9
12	Yangjian Cao, Cuiyu Township, Ninglang County, Lijiang City	YJC	100°40′23″ E	27°32′57″ N	3225	5
13	Hongqi Village, Hutiaoxia Town, Shangri-La City, Dêqên Tibetan Autonomous Prefecture	HQC	99°58′34″ E	27°21′45″ N	2957	16
14	Edi Village, Hutiaoxia Town, Shangri-La City, Dêqên Tibetan Autonomous Prefecture	ED	99°54′35″ E	27°21′22″ N	2852	5
15	Zhidu Village, Hutiaoxia Town, Shangri-La City, Dêqên Tibetan Autonomous Prefecture	ZDC	99°57′6″ E	27°20′11″ N	2771	8
16	Songhe Village, Hutiaoxia Town, Shangri-La City, Dêqên Tibetan Autonomous Prefecture	SHC	100°0′56″ E	27°19′27″ N	2941	5
17	Ludui, Jinxing Village, Hutiaoxia Town, Shangri-La City, Dêqên Tibetan Autonomous Prefecture	LD	99°59′3″ E	27°16′5″ N	2822	15
18	Yiwan Shui, Ninglang County, Lijiang City	DYW	99°49′9″ E	27°3′55″ N	3000	67
19	Mahuang Dam, Yulong Snow Mountain, Yulong County, Lijiang City	MHB	100°12′2″ E	27°2′26″ N	3310	10
20	Yuhu Village, Yulong Snow Mountain, Yulong County, Lijiang City	YHC	100°12′28″ E	27°1′44″ N	2881	9
21	Wenhai Road, Baisha Town, Yulong County, Lijiang City	WHL	100°9′36″ E	26°57′58″ N	3107	3
22	Wenhai Village, Baisha Town, Yulong County, Lijiang City	WH	100°9′36″ E	26°57′5″ N	3061	11
23	Lariguang Village, Gucheng District, Lijiang City	LRG	100°17′24″ E	26°57′45″ N	2950	8
24	Pingdiying Village, Laodian Town, Qiaojia County, Zhaotong City	PDY	103°19′48″ E	26°55′52″ N	2069	4
25	Meizi Base, Gucheng District, Lijiang City	MZ	100°18′1″ E	26°49′3″ N	2357	4
26	Wenbi Mountain, Baxi, Yulong County, Lijiang City	WBS	100°8′59″ E	26°46′12″ N	3078	3
27	Nanxi Village, Huangshan Town, Yulong County, Lijiang City	NXC	100°8′59″ E	26°46′8″ N	3103	19
28	Xiachahe Village, Yongsheng County, Lijiang City	XCH	100°51′11″ E	26°44′36″ N	2921	3

Table 1. *Cont.*

No.	Sampling Sites of Yunnan, China	Abbreviation	Longitude	Latitude	Altitude, m.a.s.l.	Number of Specimens
29	Shizhuang Village, Tangdan Town, Dongchuan District, Kunming City	SZC	102°59′57″ E	26°8′59″ N	3094	20
30	Liangwang Mountain, Chengjiang County, Kunming City	LWS	103°1′37″ E	25°25′52″ N	2780	21
31	Matou Mountain, Xiaoshao Village, Panlong District, Kunming City	XSC	102°43′42″ E	25°11′20″ N	2473	8
32	Xiaoshi Lin, Xishan District, Kunming City	XSL	102°37′56″ E	25°01′32″ N	2412	10

To minimize spatial autocorrelation, a minimum distance of 10 m was maintained between sampled individuals of the same flower color. We selected one to three representative individuals for each distinct flower color; from each individual, three fully expanded flowers were harvested, and each flower was divided evenly into two halves. One portion was allocated for color-value assessment, while the other was preserved in liquid nitrogen for laboratory analysis of pigment content studies. A total of 465 petal samples of *P. delavayi* were gathered.

2.2. Measurement of Petal Color Values

On collection day, a colorimeter (NR60CP) was used to measure and record flower color values for all samples using C/2° illuminant and Φ 4 mm aperture conditions, following the CIE color-series methodology. Two intact petals were selected from each fully expanded flower and laid flat on clean white paper with the front side facing up to avoid colored artifacts during the measurement. An additional three measurements were taken with the light-collecting port aimed at the petal center. The mean value represented the flower color of the plant [27]. The colorimeter directly measured L^*, a^*, b^*, and hue angle (h°), while chroma (C^*) was calculated as $C^* = (a^{*2} + b^{*2})^{(1/2)}$ [28].

2.3. Measurement of Petal Pigment Content

Given that white petals contain negligible pigment [29], this study focused on red-series (pink, purple-red, red, dark purple) and yellow-series (yellow, yellow-green, orange) petals. The a^* value range (a^*_{min}~a^*_{max}) of red-series petal samples and the b^* value range (b^*_{min}~b^*_{max}) of yellow-series petal samples were each divided into three equal intervals to explore the relationship between pigment composition, content and color value. For pigment content analysis, petals from individual plants representing the low-, medium-, and high-color value gradients were homogenized into a fine powder with liquid nitrogen for subsequent extraction and quantification.

2.3.1. HPLC Analysis of Anthocyanin Compounds

Extractions were made using 70% methanol (1% formic acid) and filtered through a 0.22 μm organic filter membrane. HPLC analysis conditions were as follows: column: SilgreenC$_{18}$ (4.6 mm × 250 mm, 5 μm); mobile phase: acetonitrile (A), and 0.1% formic acid aqueous solution (B); detection wavelength: 520 nm; column temperature: 30 °C; injection volume: 10 μL; flow rate: 0.8 mL/min; and gradient elution conditions: 0–10 min, 0–5% A, 10–20 min, 5–10% A, and 20–40 min, 10–20% A. The anthocyanin standards for *P. delavayi* were cyanidin-3,5-diglucoside (Cy3G5G), peonidin-3,5-diglucoside (Pn3G5G), cyanidin-3-O-glucoside (Cy3G) and peonidin-3-O-glucoside (Pn3G) [30].

2.3.2. Total Flavonoid Content Determination

For the determination of total flavonoid content, 40 μL of the sample solution was mixed with 20 μL of 50 g/L $NaNO_2$, and the mixture was incubated at 25 °C for 6 min. Thereafter, 20 μL of 100 g/L $Al(NO_3)_3$ was added, and the reaction was continued for another 6 min. Finally, 140 μL of 40 g/L NaOH solution was added to the system, with the reaction proceeding for an additional 15 min. The absorbance of the resulting mixture was immediately measured at a wavelength of 510 nm. A sample blank was prepared using the extraction solvent with the same volumes of $NaNO_2$, $Al(NO_3)_3$, and NaOH solutions under identical conditions. The absorbance values of rutin standard solutions with different mass concentrations were determined under uniform experimental conditions, and a calibration curve was constructed, with rutin mass concentration (X) as the abscissa and absorbance (Y) as the ordinate, yielding the regression equation: $Y = 0.001X + 0.0054$ ($R^2 = 0.9995$). The total flavonoid (TF) content in *P. delavayi* is quantified as milligrams of rutin equivalent per gram of fresh weight (mg RE/g FW) [31,32].

2.3.3. Determination of Photosynthetic Pigment Content

Chlorophyll and carotenoids were extracted using an 80% (*v*/*v*) acetone solution, which was prepared by mixing 80 volumes of pure acetone with 20 volumes of deionized water. The concentrations of photosynthetic pigments were determined using the following formulas [33,34]:

$$Ca = 12.7 \times A_{663} - 2.69 \times A_{645}$$

$$Cb = 22.9 \times A_{645} - 4.68 \times A_{663}$$

$$Cc = (1000 \times A_{470} - 1.82 \times Ca - 85.02 \times Cb) \div 198$$

$$CT = (C \times V) \div (M \times 1000)$$

where Ca, Cb, and Cc denote the concentrations of chlorophyll a, chlorophyll b, and carotenoids (mg/L), respectively. CT represents the concentration of chlorophyll and carotenoids (mg/g), V signifies the total volume of the extraction solution (mL), and M indicates the fresh weight of the sample (g).

2.4. Acquisition of Environmental Factor Data for Different Populations of P. delavayi

Data on annual average precipitation, temperature, and ultraviolet (UV) intensity were sourced from the National Meteorological Science Data Center (https://data.cma.cn/ (accessed on 26 June 2025)) and the Global UV-B Radiation Database (https://www.ufz.de/gluv/ (accessed on 26 June 2025)). Soil data for Yunnan Province were obtained from the National Earth System Science Data Center (http://www.geodata.cn (accessed on 26 June 2025)) of the National Science and Technology Infrastructure Platform.

2.5. Statistical Analysis

The data were stored and organized using Microsoft Excel 2010, while SPSS 27.0 was employed to perform Q-type cluster analysis on the *L**, *a**, and *b** values of all floral color samples, utilizing the farthest-neighbor (complete-linkage) method for clustering. This clustering method was selected because it generates compact clusters with clear inter-cluster boundaries, which aligns with our objective of identifying biologically meaningful flower color series with distinct phenotypic and color value characteristics in *P. delavayi*. The ColorMate 5 software converted the CIE color system values (*L**, *a**, *b**) measured by the colorimeter, into the H, V, C values of the Munsell color-series system and the corresponding color patches. These H, V, C values were then imported into the R 4.3.1 (munsellinterpol model) for processing to derive the corresponding ISCC-NBS color names,

and the Munsell color series was obtained through the Consolidated Basis of color names. Origin 2022 software was utilized for data visualization, correlation analysis, and linear regression modeling.

The quantity of samples exhibiting various color series within each sampling population of *P. delavayi* was recorded. ArcGIS 10.8.1 software was employed to extract the environmental variables of the sampling locations and to create a geographic distribution map of the distinct flower colors of *P. delavayi* populations.

3. Results

3.1. Classification of Flower Color Phenotypes in P. delavayi

3.1.1. Color Classification Based on the ISCC-NBS Color System

A total of 465 *P. delavayi* samples were categorized with color names according to the Munsell color system, yielding 54 unique color names (Table S1).

Based on the grade 3 description of the ISCC-NBS color chart method, in conjunction with the real flower color of *P. delavayi*, the brightness (V) and saturation (C) are standardized, and the hue is unified. The flower hues of *P. delavayi*, which are neither dull nor bright ($V \leq 3$, $C \leq 3.5$), are classified under the dark purple series. Consequently, nine color series are identified: yellow, yellow-green, orange-yellow, white, pink, purple-red, red, brown, and dark purple (Table 2).

Table 2. The classification of *P. delavayi* samples based on the ISCC-NBS method of designating colors.

Color Group	Sample Count	Percentage/%	CIE-Lab Color Coordinate			Munsell Color System		
			Light (*L**)	Redness/ Greenness (*a**)	Yellowness/ Blueness (*b**)	Hue (H)	Value (V)	Chroma (C)
Yellow	121	26.02%	63.75~95.47	−10.58~8.53	52.55~94.26	1.33 Y~6.94 Y	6.27~9.54	7.29~13.66
Yellow-green	22	4.72%	57.89~98.69	−23.10~−4.36	13.25~88.65	7.15 Y~3.25 GY	5.68~9.87	1.52~12.00
Orange	23	4.93%	36.38~74.79	16.54~47.91	31.75~78.31	7.59 R~8.29 YR	3.58~7.41	6.64~15.57
White	4	0.85%	93.56~95.24	−4.36~−1.84	6.13~13.25	7.13 Y~0.88 GY	9.36~9.52	0.70~0.83
Pink	4	0.85%	56.09~67.47	27.28~51.52	−1.32~14.39	5.99 RP~2.43 R	5.50~6.65	6.57~12.57
Purple-red	17	3.62%	21.67~53.27	17.87~53.44	0.53~6.57	7.92 RP~0.95 R	2.14~5.22	3.67~12.51
Red	192	40.76%	13.44~54.19	16.30~65.54	0.30~58.12	1.04 R~28.99 R	1.31~5.31	3.22~16.34
Brown	23	4.87%	6.12~55.93	7.65~49.33	5.02~45.93	6.53 R~3.09 Y	0.60~5.49	1.84~12.39
Purple-black	59	12.47%	6.53~29.38	4.02~17.36	−4.11~6.70	8.17 RP~5.69 YR	0.64~2.90	0.90~3.50

The yellow color series and red color series represent the largest proportion, indicating that these two color series are the most prevalent. In this classification scheme of the brown color series, the color name with the lowest *a** value represents strong yellowish-brown, while the color with the greatest *a** value is strong reddish-brown. Integrating yellowish-brown and reddish-brown within the brown spectrum contradicts human visual perception. Furthermore, reddish-brown constitutes a significant percentage of the brown color spectrum, and the distinction between reddish-brown and red is ambiguous when visually assessing flower colors, complicating straightforward identification of flower hues. Consequently, the exclusive use of the Munsell color-series system is insufficient for accurately characterizing the flower color of *P. delavayi*, necessitating further investigation into the classification approach for clustering analysis based on the *L**, *a**, and *b** values of *P. delavayi* flower color.

3.1.2. Color Classification Based on Cluster Analysis of *L**, *a**, and *b** Values

A cutoff line at a Euclidean distance of 10 was set to define nine distinct color series, determined solely by the inflection points of the dendrogram from the farthest-neighbor cluster analysis (Figure 1A). After obtaining the nine data-driven clusters from *L**, *a**, and *b** values, we further calibrated and named these clusters by integrating ISCC-NBS color

designations and practical visual observations of floral phenotypes. Finally, the flower colors of *P. delavayi* were categorized into nine color series (in alphabetical order): white (W), yellow (Y), yellow-green (YG), orange (O), orange-brown (OB), pink (P), red (R), purple-red (PR), and dark purple (DP) (Figure 1B). Notably, the entire clustering framework was built on pure numerical variation in Lab values, and phenotypic observations were only used for naming the pre-identified clusters and confirming their biological relevance.



Figure 1. The color classification results of *P. delavayi* flowers based on *L**, *a**, *b** values. (**A**) Cluster analysis dendrogram; horizontal axis: genetic similarity (unit: dimensionless, Euclidean distance); Roman numerals I–IX corresponding to the nine color series (W: white, Y: yellow, YG: yellow-green, O: orange, OB: orange-brown, P: pink, R: red, PR: purple-red, DP: dark purple). (**B**) Representative phenotypes of the nine *P. delavayi* color series (W, Y, YG, O, OB, P, R, PR, DP).

There were many hues that transitioned between the red and yellow series of *P. delavayi* flowers, although the red and yellow series were the most prominently represented. The data-derived cluster results fully reflected the richness of flower color variation in *P. delavayi* and were highly consistent with actual floral phenotypic observations. Specifically, the data-driven red-related clusters were assigned to red, pink, purple-red and dark purple series, yellow-related clusters to yellow, orange and yellow-green series, and the single transitional cluster between yellow and red was defined as the orange-brown series. Thus, the color series established by clustering *L**, *a**, and *b** values provides a standardized, quantitative, and repeatable standard for the classification of *P. delavayi* flower colors.

The nine *P. delavayi* color series displayed clear distinctions in color values. The lightness (*L**) values among the nine color groups varied from 6.12 to 98.69, exhibiting a coefficient of variation (*CV*) of 54.13%. The decreasing *L** values indicated the transition from lighter to darker hues: white, yellow, yellow-green, pink, orange, orange-brown, red, purple-red, and culminating in dark purple. The *L** values of orange (62.27~74.79) and yellow-green (57.89~76.84) showed minimal overlap; however, they were markedly different in their *a** values (18.65~46.47 versus −23.10~1.46, respectively). The maximum *a** value (redness) was observed in the red series (37.50~65.54), whereas the highest *b** value (yellowness) was observed in the yellow series (61.81~94.26). Despite some overlap in *a** values, white and yellow were distinctly different in their *L** and *b** values (Table 1, Figure 2). Moreover, each color series exhibited distinct distribution ranges and distinct borders in the spatial distribution plots of color values (Figure 3A,B). Consequently, the classification of color series based on cluster analysis possesses practical utility.

The flower colors of *P. delavayi* exhibited substantial coefficients of variation (51.37% to 102.05%) in the CIE-Lab system, with the *a** value demonstrating the highest coefficient of variation (102.05%), followed by the *b** value (94.37%). This indicates a significant degree

of variability in flower color features among various plants, particularly highlighting remarkable distinctiveness and variation in red-hued petals.

A two-dimensional scatter plot depicting L^* and C^* values for *P. delavayi* flower hues was generated, with a fitted linear regression equation: $L^* = 0.8148\ C^* + 7.3155$ ($R^2 = 0.6432$) (Figure 3C). The model fitness was satisfactory (Pearson's r = 0.8025, $R^2 = 0.6432$), where R^2 represents the coefficient of determination, which indicates the strength of linear model fitness, revealing a significant positive correlation between L^* and C^* values.

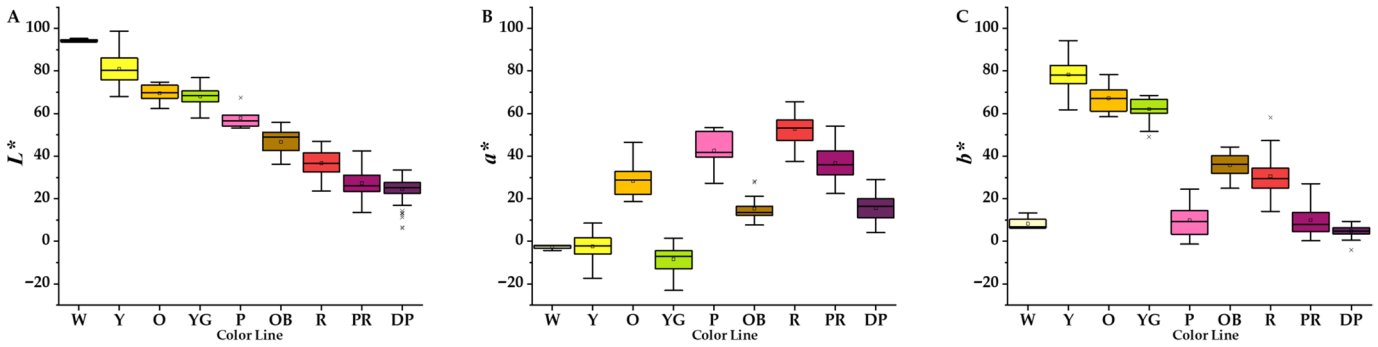


Figure 2. Boxplots of nine color of *P. delavayi* lines based on clustering analysis of L^* (**A**), a^* (**B**) and b^* (**C**) values. Different colored boxes represent the nine distinct color series of *P. delavayi* (W: white, Y: yellow, YG: yellow-green, O: orange, OB: orange-brown, P: pink, R: red, PR: purple-red, DP: dark purple).

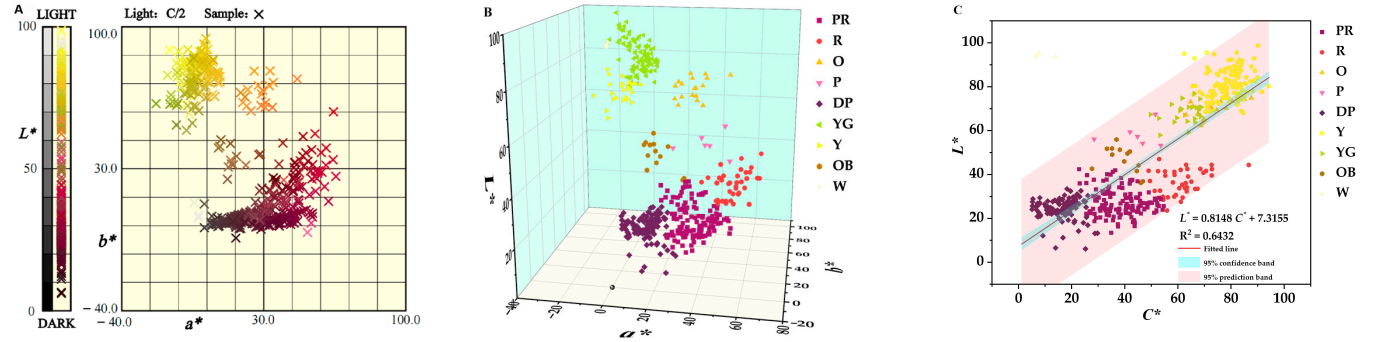


Figure 3. Color value spatial distribution maps of different color series of *P. delavayi*. (**A**) Two distribution scatter plots of a^* and b^* values. (**B**) Three distribution scatter plots of L^*, a^*, and b^* values. (**C**) Two-dimensional distribution diagram of C^* and L^* values for all flower color samples of *P. delavayi*.

3.2. Pigment Determination in P. delavayi Petals and Correlation Analysis with Color Values

Data analysis indicated that the pigment composition and content of red and yellow petal color groups differ markedly (Figures 4 and 5), and were distinctly correlated with petal color values, with 73 sets of data exhibiting significant correlation ($p < 0.05$) (Figure 6).

Total flavonoids (TF) content was high in both the red series (67.78 ± 2.73 mg RE/g FW) and yellow series (63.56 ± 1.79 mg RE/g FW) petals, with little numerical difference between the two color groups (Figure 4A). TF content exhibited a significant positive correlation with the a^* value (r = 0.36, $p < 0.05$) (Figure 6).

The yellow-green-series petals exhibited the highest chlorophyll concentration (Figure 4B,C), which demonstrated a significant negative correlation with the a^* value (redness) (r = −0.74, $p < 0.01$) and a significant positive correlation with the hue angle (h°) (r = 0.81, $p < 0.01$) (Figure 6). The orange-series petals exhibited the highest carotenoid concentration (0.72 ± 0.004 mg/g FW) (Figure 4D), although no significant correlation with color values was observed ($|r| < 0.44$, $p > 0.05$) (Figure 6).

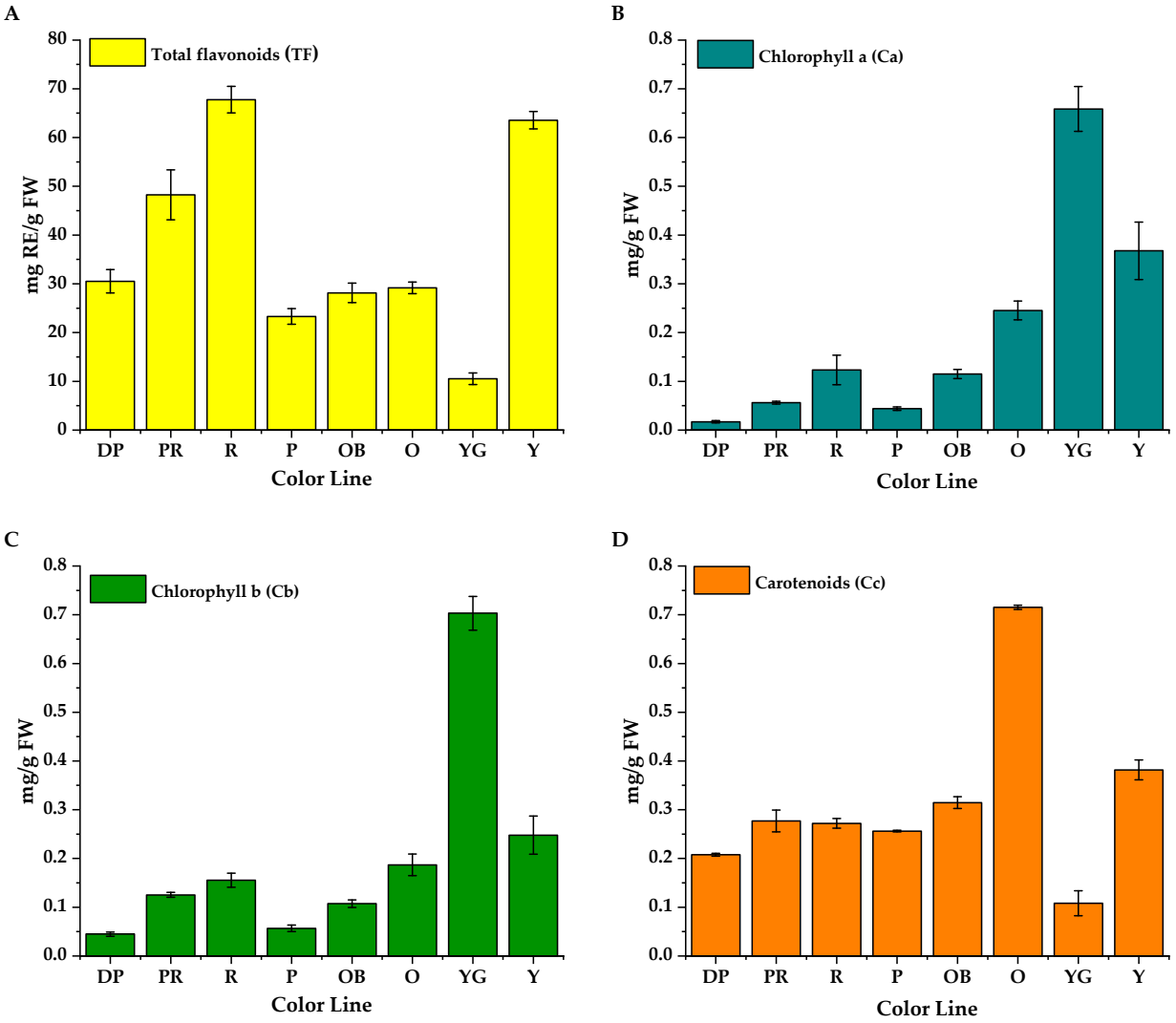


Figure 4. Total flavonoids (TF) (**A**), chlorophyll a (Ca) (**B**), chlorophyll b (Cb) (**C**), and carotenoid (Cc) (**D**) content in different flower colors of *P. delavayi* (average ± SD).

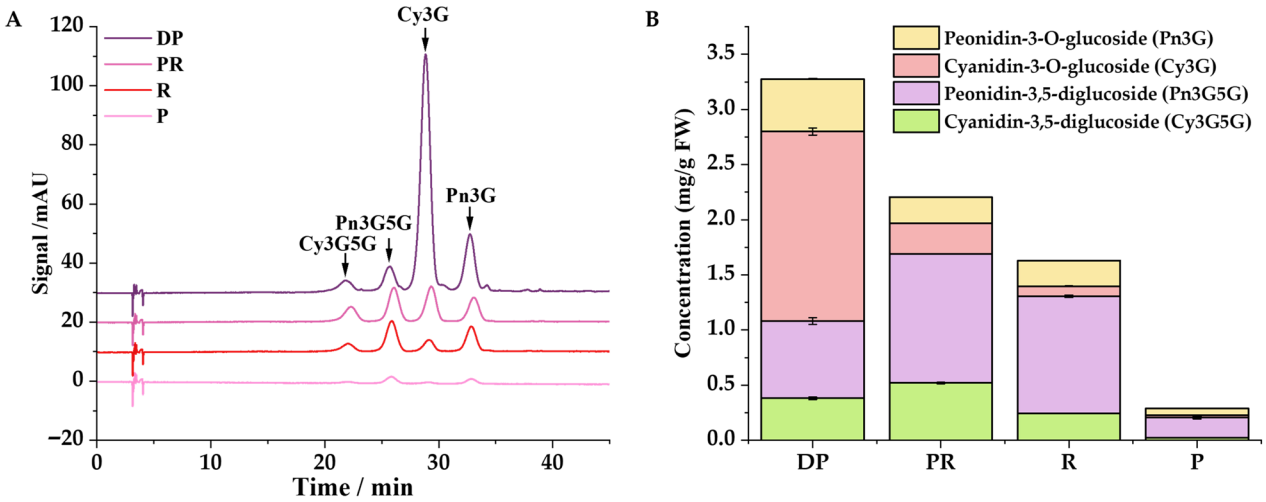


Figure 5. HPLC chromatograms (**A**), and content analysis (average ± SD) (**B**) of anthocyanins in flowers of *P. delavayi* with different color phenotypes: deep purple (DP), purplish-red (PR), red (R), and pink (P).

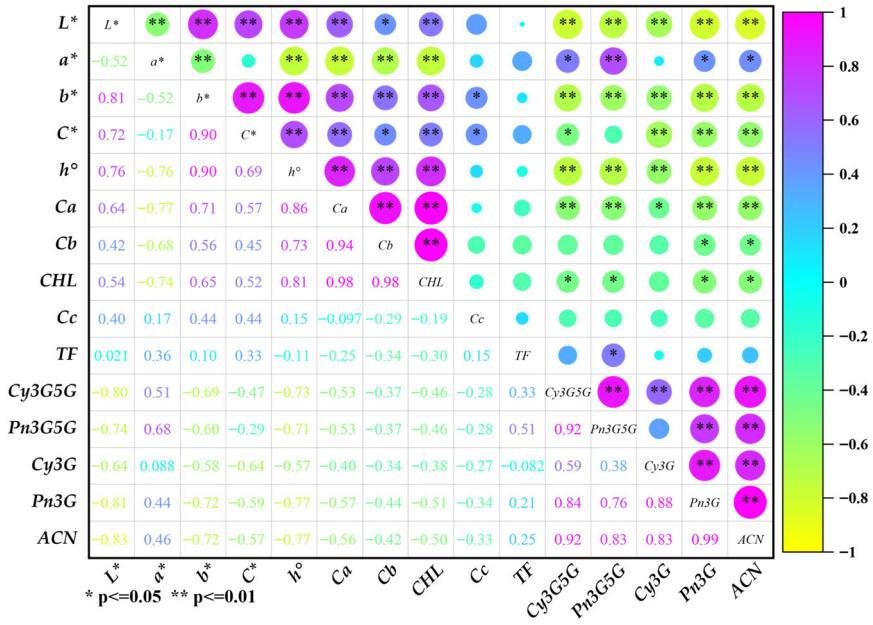


Figure 6. Correlation analysis between color values and pigments in *P. delavayi*.

Anthocyanins were identified in the petals of the red color series (Figure 5A). Their overall content increased markedly with decreasing lightness (L^*), in the following sequence: dark purple series > purple-red series > red series > pink series (Figure 5B). The total anthocyanin content (ACN) exhibited a highly significant negative correlation with lightness (L^*) ($r = -0.83$, $p < 0.01$) and a significant positive correlation with redness (a^*) ($r = 0.46$, $p < 0.05$) (Figure 6). For red-series petals, anthocyanin (ACN) and total flavonoid (TF) contents exhibited strong quantitative associations with key color values, leading to the development of highly reliable predictive models. Specifically, the linear regression model between ACN and lightness (L^*) yielded an R^2 of 0.896 (Pearson's $r = -0.946$), while the model between TF and redness (a^*) achieved an R^2 of 0.648 (Pearson's $r = 0.805$) (Figure 7A,B). Chlorophyll (CHL) content in yellow-green petals showed a strong negative correlation with a^* values ($r = -0.740$, $p < 0.01$) and a positive correlation with hue angle (h°, $r = 0.810$, $p < 0.01$), with its predictive model (CHL vs. a^*) reaching an R^2 of 0.548 (Figure 7C). These equations provide non-destructive, rapid estimation of pigment contents from easily measured color parameters, offering practical applications for large-scale germplasm screening and color-targeted breeding in *P. delavayi*.

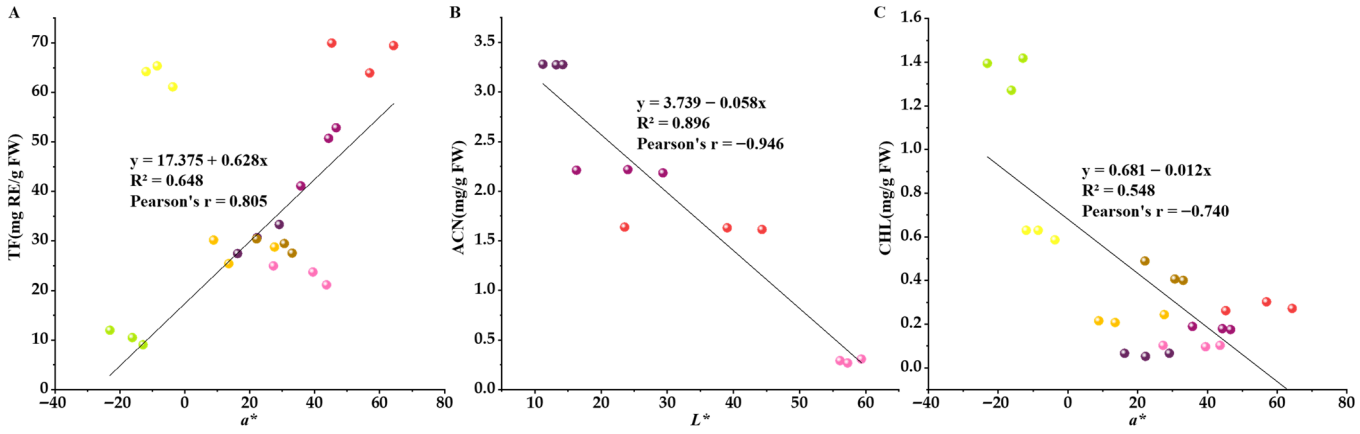


Figure 7. Correlation prediction models of (**A**) total flavonoids (TF) vs. a^* ($R^2 = 0.648$), (**B**) total anthocyanins (ACN) vs. L^* ($R^2 = 0.896$), and (**C**) total chlorophyll (CHL) vs. a^* ($R^2 = 0.548$) in *P. delavayi*.

3.3. Influence of Environmental Factors on Flower Color Variation in *P. delavayi*

The examination of geo-climatic parameters demonstrated a notable association with the spatial distribution of *P. delavayi* flower colors. The HXC population at Shangri-La displayed the greatest color richness, comprising eight distinct color groups, followed by the populations LZ and LZSK in Lijiang, each comprising five color series (Figure 8). The GZ and Yangla populations in Shangri-La were observed to have the rare white series, with yellow-green and yellow variants. In sharp contrast, populations in Dêqên County (e.g., YRC, BM7, SSC, GHT, ED, HQC, SHC) were monomorphic, consisting solely of the yellow color series. The populations in Yulong County (e.g., NX, WH, YHC) were consistently identified as belonging to the red color series. A significant lack of diversity was noted in central and northeastern Yunnan (Kunming and Zhaotong), where populations were largely dominated by yellow-series phenotypes (Y, YG).

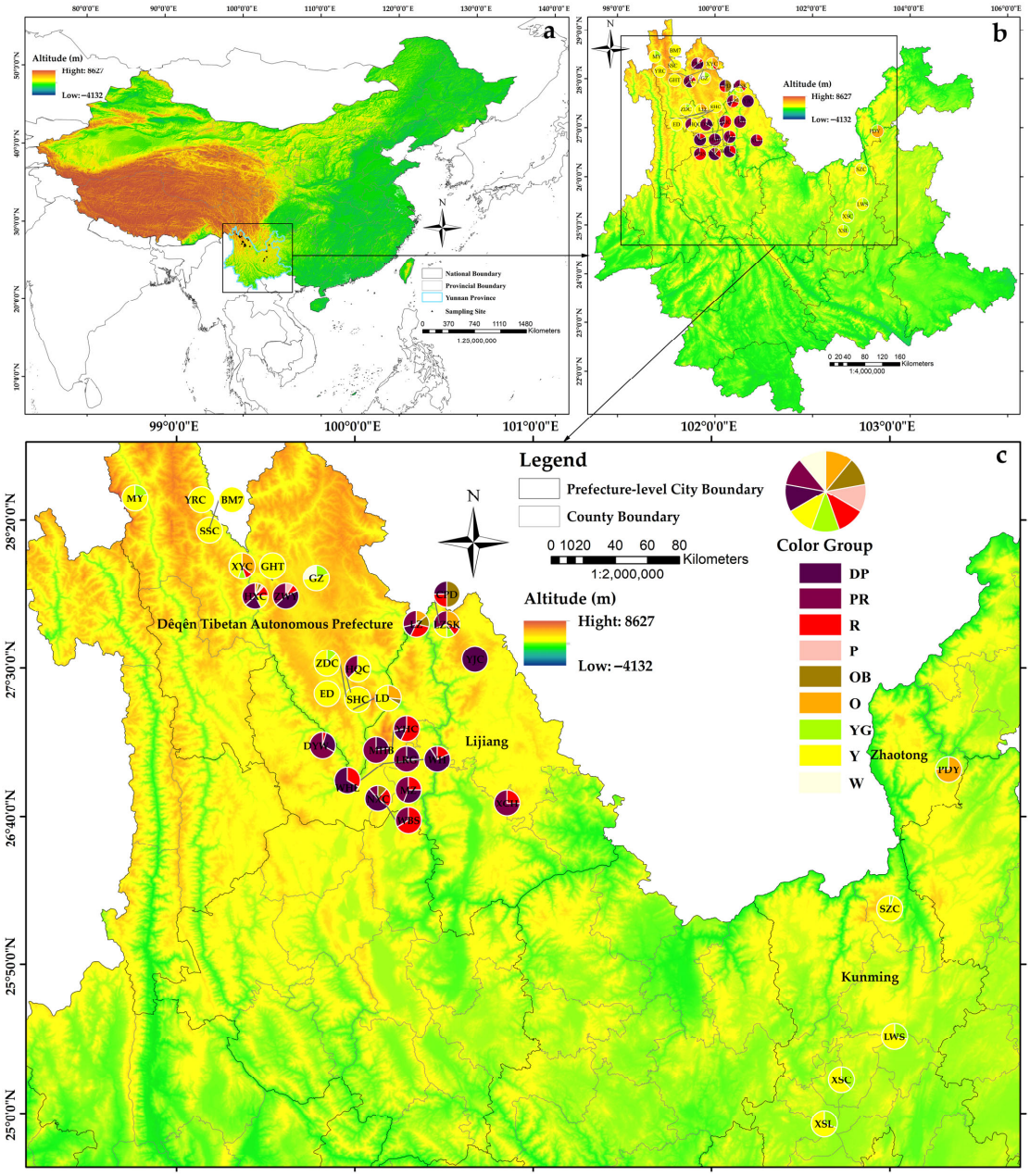


Figure 8. Distribution map of flower colors of *P. delavayi* in Yunnan province, China. (**a**) Location of Yunnan Province in China (black box). (**b**) Topographic map of Yunnan, with the detailed study area outlined by a black box. (**c**) Detailed distribution of *P. delavayi* populations and their flower color groups.

Spearman correlation analysis identified specific environmental niches associated with color patterns (Figure 9). Habitats that promote high color diversity were defined by low mean annual temperature (MAT: 4.2–8.1 °C), moderate-to-high annual precipitation (APA: 698–805 mm), moderate-to-high ultraviolet radiation (UV-B: 6044–6248 kJ/m^2·day), and gentle slopes (<15°). The HXC population, situated at an altitude of 3360 m with a mean annual temperature of 4.2 °C, an annual precipitation of 698 mm, and a slope of 6.3°, exemplifies this phenomenon, exhibiting the largest diversity. Populations in warmer Lijiang (MAT > 7.5 °C; e.g., WH, MZ, CPD) were primarily composed of the red series (R, PR, DP). In contrast, the broad thermal range in central Yunnan (MAT: 1.3–14.8 °C; e.g., LWS, XSL, PDY) led to the sole predominance of the yellow series (Y, YG). The white series (W) was strongly associated with the high-UV, low-MAT conditions of the GZ population (elevation 3186 m; MAT 4.9 °C; UV-B 6248 kJ/m^2·day). A thermal threshold was apparent, with only the yellow series enduring in regions where the mean annual temperature surpassed 12 °C (e.g., XSL, XSC). Steeper slopes (>20°) were associated with reduced variety, as evidenced by the monomorphic yellow-series composition of the BM7 population (slope 29.7°).

The distribution of dark-colored flowers (DP, PR, R) exhibited a significant positive link with high-altitude and nutrient-rich soils, characterized by higher soil organic carbon (SOC) and total nitrogen (STN). This indicates an adaptive response to high-altitude stresses such as elevated UV radiation, facilitated by sufficient food availability for pigment production. The presence of the yellow series (Y, YG) was associated with lower elevations and less UV exposure. Their distribution was markedly constrained by elevated MAT, presumably suggesting heat sensitivity in the carotenoid production pathway. Pink flowers (P) exhibited a preference for cool (low mean annual temperature), high-precipitation (high annual precipitation), and low-slope environments. Increased soil pH typically inhibited red-series expression, probably due to the pH-dependent instability of anthocyanin pigments.

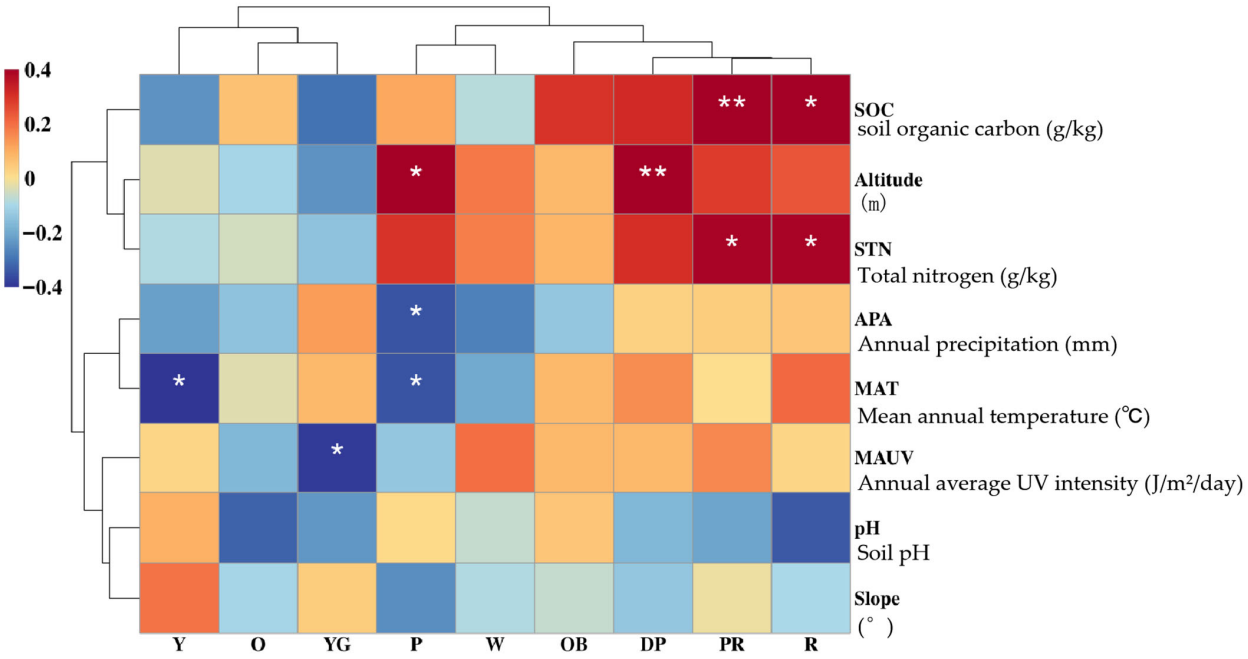


Figure 9. Correlation heatmap between geographic–climatic factors and flower color variations in *P. delavayi*. The abbreviations in the legend are defined as follows: SOC, soil organic carbon (g/kg); STN, total nitrogen (g/kg); APA, annual precipitation (mm); MAT, mean annual temperature (°C); MAUV, annual average UV intensity (J/m^2/day); pH, soil pH. The color gradient represents the Pearson correlation coefficient, ranging from −0.4 (blue, negative correlation) to 0.4 (red, positive correlation). Asterisks indicate significant correlations: * $p < 0.05$, ** $p < 0.01$.

4. Discussion and Conclusions

The CIE-Lab color system and cluster analysis quantitatively characterized the diversity of flower colors in *P. delavayi*, categorizing them into nine distinct color series with defined boundary values: white (W), yellow (Y), orange (O), yellow-green (YG), pink (P), orange-brown (OB), red (R), purple-red (PR), and dark purple (DP). The farthest-neighbor linkage method ensured that each of the nine color series had non-overlapping L^*, a^*, b^* value ranges (Table 3) and distinct biochemical profiles, confirming that the clustering method is well-suited for identifying biologically meaningful flower color series in *P. delavayi.* This establishes a reference color standard for studying flower color phenotypes in *P. delavayi* and other ornamental species. This study presents a nine-color series defined by color values, establishing a standardized framework of color values, in contrast to earlier qualitative descriptions of *P. delavayi* flower colors, which identified ten colors: yellow, orange, variegated, red, purple-red, purple, dark purple, yellow-green, pink, and green [15], or seven colors (green, yellow, yellow-green, light yellow, orange-yellow, purple-red, and dark red)—classified according to the RHSCC system [14]. The dark purple series delineated in this work approximates the previously described purple, dark purple, and dark red petals while providing distinct color value indications, so enhancing communication and discourse in floral color research.

Table 3. Distribution range of L^*, a^* and b^* values of each color group in *P. delavayi* based on cluster analysis.

Color Group	Sample Count	Percentage/%	Light (L^*)	Redness/ Greenness (a^*)	Yellowness/ Blueness (b^*)	Chroma (C^*)	Hue (h°)
White	4	0.86%	93.56~95.24	−4.36~−1.84	6.13~13.25	6.52~13.95	104.13~109.83
Yellow	119	25.59%	67.98~98.69	−17.37~8.53	61.81~94.26	62.40~94.27	83.32~102.85
Orange	18	3.87%	62.27~74.79	18.65~46.47	58.49~78.31	63.09~87.64	57.98~74.56
Yellow-green	24	5.16%	57.89~76.84	−23.10~1.46	49.01~68.50	49.67~68.71	88.72~110.40
Pink	6	1.29%	53.27~67.41	27.28~53.44	−1.32~24.49	28.47~53.54	−1.47~31.59
Orange-brown	13	2.80%	36.24~55.93	7.65~28.24	24.91~44.33	27.69~46.82	52.90~79.25
Red	39	8.39%	23.55~47.03	37.50~65.54	14.00~58.12	48.98~86.68	12.75~47.36
Purple-red	134	29.03%	13.44~42.40	22.42~54.07	0.30~27.04	22.79~54.67	0.60~36.45
Dark purple	108	23.44%	6.12~33.43	4.02~29.08	−4.11~9.33	5.11~29.71	−14.20~56.59
Mean			46.41	19.63	33.56	48.02	45.11
CV/%			54.13%	102.05%	94.37%	51.37%	79.53%
SD			1.16	0.93	1.47	1.14	1.67

This study offers a cohesive, reproducible quantitative standard, in contrast to the ambiguous categorization of reddish-brown and orange-brown as a "brown series" in the Munsell system, which may introduce visual cognitive bias. Establishing the ranges of L^*, a^*, and b^* values substantially enhances the precision of flower color identification and communication, thereby providing a basis for studying correlations among pigment content, environmental conditions, and quantitative color values. This also gives a theoretical foundation for further elucidating its genetic mechanisms and ecological significance, providing evidence of the substantial genetic variety present in *P. delavayi.*

The petals of *P. delavayi* exhibit significant color diversity, with a broad spectrum of color values a^* (−23.10 to 65.54) and b^* (−4.11 to 94.26), alongside substantial coefficients of variation (51.37% to 102.05%). This pattern illustrates the extensive diversity of flower colors in *P. delavayi*, highlighting the intricacy of its floral color characteristics and the significant natural variance in color values, indicating a high level of genetic diversity. This corresponds with its significance as vital germplasm for ornamental peony breeding (e.g., yellow cultivars) and its capacity to acclimatize to several habitats, providing a crucial genetic foundation for its application in ornamental plant breeding. The variation in petal color and its spectrum of hues is attributable to the interplay of different types and

concentrations of secondary metabolite pigments [35]. The correlation between various color series and distinct pigment composition and content suggests that the attributes of pigment composition and content serve as the biological foundation for variations in petal color. Various flower pigment types arise from disparities in biosynthetic metabolism, illustrating the variation and diversity in metabolic pathways among plants with differently colored petals.

Total flavonoids (TF) are predominantly distributed in the yellow- and red-series petals of *P. delavayi*. Flowers exhibiting yellow, yellow-green, or orange coloration appear to depend primarily on the presence of carotenoids and chlorophyll, with anthocyanins generally undetectable. In contrast, the coloration of red, purple-red, and dark purple petals is closely associated with anthocyanin accumulation, which tends to coincide with reduced L^* and increased a^*. Yellow-series petals, characterized by elevated b^* values, typically lack anthocyanins; their coloration may be influenced by the relative proportions of total flavonoids, carotenoids, and chlorophyll. Among these, the orange series shows the highest carotenoid levels, while the yellow-green series exhibits the highest chlorophyll content. In the yellow-green series, chlorophyll concentration shows a strong negative correlation with a^* values and a positive correlation with hue angle, suggesting that chlorophyll may play a role in modulating the pigmentation of yellow-green petals, possibly by affecting light absorption and reflection within petal tissues. This observation is consistent with previous studies on chrysanthemums [36,37] and *P. delavayi* [38,39], which have indicated that chlorophyll can contribute to greenish-yellow hues in petals.

While anthocyanins are widely recognized as important pigments associated with red and purple hues in flowering plants [40,41], this study attempts to extend beyond correlative observations by developing quantitative models that link color phenotypes with pigment composition. For red-series petals, the anthocyanin–L^* model ($R^2 = 0.896$) and the total flavonoid–a^* model ($R^2 = 0.652$) suggest a potential quantitative relationship between these pigments and chromatic traits. Such models may offer a useful reference for breeding applications, as they provide a means to estimate pigment content from colorimeter readings, potentially facilitating the selection of breeding materials with desired color–pigment characteristics [42]. Further validation across a wider range of germplasm and environmental conditions would be necessary to assess the general applicability of these models. Overall, a more quantitative understanding of the relationship between petal color and pigment composition may contribute to the interpretation of genetic and ecological aspects of floral coloration, and may help clarify the basis of phenotypic variation observed in *P. delavayi*.

The regional distribution of *P. delavayi* plants exhibiting various petal colors demonstrates significant relationships with environmental conditions. The HXC population in Shangri-La exhibited all eight non-white color series, demonstrating the greatest diversity in flower coloration; the LZ and LZSK populations in Lijiang also displayed comparatively high flower color diversity; *P. delavayi* specimens found in the lower-altitude central Yunnan region predominantly feature yellow and yellow-green petals. Data from 543 specimen records in the digital herbarium and relevant literature suggest that yellow-series petal plants were documented in central Yunnan only [43]. After more than ten years of research and investigation, the research team has documented exclusively yellow-series plants in central Yunnan. This indicates that the elevated regions of northern Yunnan, specifically the Shangri-La–Li-jiang area, exhibit the most vibrant floral hues of *P. delavayi* and serve as the center of its floral color diversity. This distribution pattern may arise from the combined influences of high altitude, low temperature, and elevated ultraviolet radiation within the intricate and varied mountain ecological habitat. Flower color traits may be affected by variables such as light intensity, temperature, and soil conditions in the environment,

resulting in notable variation in flower color among distinct populations or individuals due to environmental changes [44,45]. Data analysis indicates that, in environments characterized by low temperatures (mean annual temperature 4.2–8.1 °C), moderate-to-high precipitation (698–805 mm), moderate-to-high ultraviolet radiation (6044–6248 kJ/m^2·day), and gentle slopes (slope < 15°), the floral color diversity of *P. delavayi* at the Shangri-La Shika Snow Mountain area is maximized (e.g., HXC). These environmental conditions may jointly facilitate the development and preservation of flower color variation in this region by influencing gene expression, enzyme activity, or natural selection pressure. The yellow series tolerates a broader temperature range (1.3–14.8 °C), but the red series (R, PR, DP) is predominantly found in the Lijiang region, where the mean annual temperature typically exceeds 7.5 °C. Conversely, the floral color composition of populations in central and northeastern Yunnan (Kunming, Zhaotong) is generally homogeneous, consisting predominantly of yellow variants (Y, YG). *P. delavayi* is found in mountainous regions at elevations ranging from 2000 m to 4000 m above sea level, exhibiting a broad altitudinal range and a variety of habitat types indicative of its extensive ecological niche and robust adaptation. Moreover, the habitats of *P. delavayi* generally consist of sunlit slopes, forest margins, and shaded rocky hills, demonstrating its broad ecological tolerance for light, capacity to acclimatize to varying light levels, and a degree of shade tolerance [46]. *P. delavayi* exhibits morphological and structural adaptations to many habitats, allowing it to thrive in complex ecological contexts and demonstrating its adaptive ability and methods for diverse environmental situations.

Analysis of the correlation between the distribution of flower colors and ecological factors provides a basis for comprehending the causes of the geographical distribution pattern of *P. delavayi* flower colors. The pronounced positive association between dark flower colors (DP, PR, R) and elevated altitude and high soil nutrient levels (SOC, STN) is noteworthy. High-altitude environments are typically characterized by elevated ultraviolet (UV-B) radiation and thermal stress. The photoprotective role of anthocyanins constitutes a significant antioxidant mechanism, diminishing the generation of reactive oxygen species (ROS) at the origin and safeguarding plant cells from photodamage [47]. However, we acknowledge that such phenotypic–environment correlations may alternatively reflect neutral processes such as genetic drift (e.g., founder effects) in isolated mountain populations, rather than adaptive responses. The production of secondary metabolites, such as anthocyanins, is a process that requires significant energy consumption [48]; fertile soil (high SOC, STN) can supply adequate carbon and nitrogen sources, facilitating the development and sustenance of dark phenotypes from a resource allocation standpoint. This closely aligns with the diverse floral color spectrum found in high-altitude regions with healthy soil, such as HXC in Shangri-La. Conversely, yellow series flower colors (Y, YG) correlate with lower altitudes and diminished UV light, and their distribution is markedly constrained by elevated mean annual temperature (MAT). Whether this thermal constraint reflects adaptive limitation of carotenoid metabolism or simply demographic history of source populations remains to be tested. Elevated soil pH typically suppresses red hues in flowers, potentially due to anthocyanin chemical stability [49]. The spatial distribution of *P. delavayi* flower colors is likely shaped by the combined effects of environmental selection and genetic drift. While the significant correlations between dark flower colors and high-altitude/nutrient-rich environments support a role for environmental filtering, we cannot exclude the contribution of genetic drift in isolated mountain populations. Distinguishing between these mechanisms will require future population genomic studies. This balanced perspective is consistent with findings in *Primula vulgaris*, where floral color diversity is shaped by the combined action of evolutionary forces including environmental selection and genetic drift [50].

The vast variation of flower colors in *P. delavayi* reflects its genetic capacity and adaptation to the intricate ecological conditions of high-altitude plateaus and mountains. It offers valuable resources for the genetic enhancement of peony flower color and the preservation of germplasm. The diverse traits of *P. delavayi* offer significant germplasm resources for comprehensive investigation of the relationship between flower color development and ecological adaptability, the study of its molecular mechanisms, and the optimization of its potential applications in ecological conservation and the horticultural sector. Designating the high-altitude regions of northern Yunnan as the center of floral color diversity and a repository of genetic resources provides a crucial scientific foundation for developing measures to conserve the genetic diversity of *P. delavayi*. It provides fundamental data for developing strategies to prioritize the safeguarding of high-diversity hotspots (e.g., HXC and its vicinity), so ensuring the successful conservation of its abundant genetic resources and potential adaptive variants.

Supplementary Materials: The following supporting information can be downloaded at: https://www.mdpi.com/article/10.3390/d18030164/s1. Table S1 The color names of 465 *P. delavayi* flower samples based on the ISCC-NBS system.

Author Contributions: Data collection and experimental analysis: S.L., H.L. and J.W.; Experimental assistance: C.D. and J.L.; Translation and proofreading: G.H. and J.W.; Supervising of manuscript preparation: J.W., Y.P. and J.X. All authors have read and agreed to the published version of the manuscript.

Funding: This research was supported by "10000 Talent Plan" of Yunnan Province in China ([2018]212), the Digitalization, Development and Application of Biotic Resource of the Science and Technology Planning Project of Yunnan Province (202002AA100007), the Scientific Research Fund Project of Yunnan Provincial Department of Education (2020Y0412), and National Natural Science Foundation of China (32060089).

Data Availability Statement: The original contributions presented in the study are included in the article/Supplementary Material. Further inquiries can be directed to the corresponding author.

Acknowledgments: We are grateful to all members of our research group for their assistance in field investigations and laboratory analyses. Special thanks are also due to the funding agencies that supported this work.

Conflicts of Interest: The authors declare no conflicts of interest.

Abbreviations

The following abbreviations are used in this manuscript:

Pn3G	Peonidin-3-O-glucoside
Cy3G	Cyanidin-3-O-glucoside
Pn3G5G	Peonidin-3,5-diglucoside
Cy3G5G	Cyanidin-3,5-diglucoside
ACN	Total Anthocyanin
TF	Total Flavonoid
CHL	Chlorophyll
SOC	Soil Organic Carbon
STN	Soil Total Nitrogen
MAT	Mean Annual Temperature
APA	Annual precipitation
MAUV	annual average UV intensity
CHS	Chalcone Synthase
DFR	Dihydroflavonol 4-Reductase
ANS	Anthocyanidin Synthase

PSY	Phytoene Synthase
LCD	Lycopene Cyclase D

References

1. Zhou, S.L.; Xu, C.; Liu, J.; Yu, Y.; Wu, P.; Cheng, T.; Hong, D.Y. Out of the Pan-Himalaya: Evolutionary history of the Paeoniaceae revealed by phylogenomics. *J. Syst. Evol.* **2021**, *59*, 1170–1182. [CrossRef]
2. National-Forestry-and-Grassland-Administration. Announcement by the National Forestry and Grassland Administration and the Ministry of Agriculture and Rural Affairs of the Central People's Government of the People's Republic of China. Available online: https://www.forestry.gov.cn/c/www/lczc/10746.jhtml (accessed on 7 May 2024).
3. Hong, D.Y.; Zhou, Q.L.; He, S.; He, X.J.; Yuan, J.H.; Zhang, Y.L.; Cheng, F.Y.; Zeng, X.L.; Wang, Y. The Survival Status and Conservation of Wild Tree Peonies. *Biodivers. Sci.* **2017**, *25*, 781–793. (In Chinese) [CrossRef]
4. Gong, X.; Pan, Y.Z.; Yang, Z.Y. The diversities and value of present situation of *Paeonia delavayi*. *Acta Bot. Boreali-Occident. Sin.* **2003**, *23*, 218–223. (In Chinese)
5. Zou, H.Z.; Zhou, L.; Han, L.L.; Lv, J.H.; Jia, Y.H.; Wang, Y. Transcriptome profiling reveals the roles of pigment formation mechanisms in yellow *Paeonia delavayi* flowers. *Mol. Genet. Genom.* **2022**, *298*, 375–387. [CrossRef] [PubMed]
6. Wang, L.Y.; Yuan, T.; Li, Q.D.; Zhao, X.Z. *Illustrated Catalogue of Chinese Peony Varieties: Supplement*; China Forestry Publishing House: Beijing, China, 2015; pp. 2–16. (In Chinese)
7. Yuan, T.; Wang, L.Y. Morphological Studies on *Paeonia* Sect. *Moutan* Subsect *Vagiatae* in China. *Acta Hortic. Sin.* **2003**, *2*, 187–191. (In Chinese) [CrossRef]
8. Li, S.F.; Cai, Y.F.; Zhang, X.X.; Xue, J.Q.; Xiong, C.K.; Zhai, S.P. Phenotypic Diversity of Natural Populations of *P. delavayi*. *Southwest China J. Agric. Sci.* **2016**, *29*, 2470–2478. (In Chinese) [CrossRef]
9. Zhang, X.X.; Sun, J.Y.; Niu, L.X.; Zhang, Y.L. Chemical Compositions and Antioxidant Activities of Essential Oils Extracted from the Petals of Three Wild Tree Peony Species and Eleven Cultivars. *Chem. Biodivers.* **2017**, *14*, e1700282. [CrossRef]
10. Yan, Z.G.; Xie, L.H.; Tian, Y.; Li, M.C.; Ni, J.; Zhang, Y.L.; Niu, L.X. Insights into the Phytochemical Composition and Bioactivities of Seeds from Wild Peony Species. *Plants* **2020**, *9*, 729. [CrossRef]
11. Zhang, J.M.; Liu, J.; Sun, H.L.; Yu, J.; Wang, J.X.; Zhou, S.L. Nuclear and chloroplast SSR markers in *Paeonia delavayi* (Paeoniaceae) and cross-species amplification in *P. ludlowii*. *Am. J. Bot.* **2011**, *98*, e346–e348. [CrossRef]
12. Xue, Y.Q.; Liu, R.; Xue, J.Q.; Wang, S.L.; Zhang, X.X. Genetic diversity and relatedness analysis of nine wild species of tree peony based on simple sequence repeats markers. *Hortic. Plant J.* **2021**, *7*, 579–588. [CrossRef]
13. Zhao, Y.J.; Yin, G.S.; Pan, Y.Z.; Tian, B.; Gong, X. Climatic Refugia and Geographical Isolation Contribute to the Speciation and Genetic Divergence in Himalayan-Hengduan Tree Peonies (*Paeonia delavayi* and *Paeonia ludlowii*). *Front. Genet.* **2021**, *11*, 595334. [CrossRef]
14. Zhang, Y.L.; Li, Z.H.; Ma, H.; Wang, Y.; Li, W.J.; Liu, X.X.; Wan, Y.M. Character Variation of Flower Color Groups in *P. delavayi* Franch. *Plant Divers.* **2011**, *33*, 183–190. (In Chinese)
15. Wang, X.Q. Studies on Genetic Diversity of *P. delavayi* in Shangri-la. Ph.D. Thesis, Beijing Forestry University, Beijing, China, 2009.
16. Phillip, C.P.; Mark, A.S. Measuring Camellia Petal Color Using a Portable Color Sensor. *Horticulturae* **2020**, *6*, 53. [CrossRef]
17. Gonnet, J.F. CIELab measurement, a precise communication in flower colour: An example with carnation (*Dianthus caryophyllus*) cultivars. *J. Hortic. Sci.* **2015**, *68*, 499–510. [CrossRef]
18. Cochrane, S. The munsell color system: A scientific compromise from the world of art. *Stud. Hist. Philos. Sci. Part A* **2014**, *47*, 26–41. [CrossRef]
19. Kelly, K.L.; Judd, D.B. *Color Universal Language and Dictionary of Names*; U.S. Department of Commerce, National Bureau of Standards: Washington, DC, USA, 2018; pp. 1–19.
20. Ji, K.M.; Xue, Y.Q.; Cui, Z.X. A new method for colors characterization of colored stainless steel using CIE and Munsell color systems. *Opt. Mater.* **2015**, *47*, 180–184. [CrossRef]
21. Boronkay, G.; Hamar-Farkas, D.; Kisvarga, S.; Békefi, Z.; Neményi, A.; Orlóci, L. Developing a Colorimetrically Balanced, Measurement-Based Petal Colour System for Cultivated Rose (*Rosa* L. Cultivars) and the Resulting Colour Categories. *Plants* **2024**, *13*, 1368. [CrossRef] [PubMed]
22. Cui, H.L.; Zhang, Y.N.; Shi, X.L.; Gong, F.F.; Xiong, X.; Kang, X.P.; Xing, G.M.; Li, S. The numerical classification and grading standards of daylily (*Hemerocallis*) flower color. *PLoS ONE* **2019**, *14*, e0216460. [CrossRef]
23. Lu, C.F.; Li, Y.F.; Wang, J.Y.; Qu, J.P.; Chen, Y.; Chen, X.Y.; Huang, H.; Dai, S.L. Flower color classification and correlation between color space values with pigments in potted multiflora chrysanthemum. *Sci. Hortic.* **2021**, *283*, 110082. [CrossRef]
24. Zhou, Y.W.; Mao, Y.; Farhat, A.; Sun, Y.; Gao, T.; Yan, F.L.; Li, X.Y.; Yu, Y.Y.; Yue, Y.C.; Yu, R.C.; et al. Classification and Association Analysis of Gerbera (*Gerbera hybrida*) Flower Color Traits. *Front Plant Sci.* **2021**, *12*, 779288. [CrossRef]

25. Guo, X.; Cheng, F.Y.; Zhong, Y.; Chen, X.Y.; Tao, X.W. The Quantitative Classification of Flower Color Phenotype in *Paeonia rockii* (Flare Tree Peony). *Acta Hortic. Sin.* **2022**, *49*, 86–99. (In Chinese) [CrossRef]
26. Li, Y.X.; Liu, H.Y.; Li, Z.; Liu, P.; Hao, Q. The analysis of flower color phenotype in tree peony. *Liaoning For. Sci. Technol.* **2018**, 1–6. (In Chinese)
27. Wang, S.Y.; Zhang, G.; Yang, S.C.; Jiang, S.L.; Wang, R.H.; Wang, J. Numerical Classification of Phalaenopsis Flower Colour Based on Phenotype. *Chin. J. Trop. Crops* **2023**, *44*, 2227–2235.
28. Wang, L.S.; Fumio, H.; Aya, S.; Noriaki, A.; Li, J.J.; Sakata, Y. Chemical taxonomy of the Xibei tree peony from China by floral pigmentation. *J. Plant Res.* **2004**, *117*, 47–55. [CrossRef]
29. Wang, H.; Fan, Y.; Yang, Y.; Zhang, H.; Li, M.; Sun, P.; Zhang, X.; Xue, Z.; Jin, W. Classification of rose petal colors based on optical spectrum and pigment content analyses. *Hortic. Environ. Biotechnol.* **2022**, *64*, 153–166. [CrossRef]
30. Wang, J.; Lewis, D.; Shi, R.; McGhie, T.; Wang, L.; Arathoon, S.; Schwinn, K.; Davies, K.; Qian, X.H.; Zhang, H.B. The colour variations of flowers in wild *Paeonia delavayi* plants are determined by four classes of plant pigments. *N. Z. J. Crop Hortic. Sci.* **2021**, *50*, 69–84. [CrossRef]
31. Wang, Z.X.; Jin, X.M.; Zhang, X.C.; Xie, X.; Tu, Z.C.; He, X.H. From Function to Metabolome: Metabolomic Analysis Reveals the Effect of Probiotic Fermentation on the Chemical Compositions and Biological Activities of *Perilla frutescens* Leaves. *Front. Nutr.* **2022**, *9*, 933193. [CrossRef]
32. Sari, K.R.P.; Ikawati, Z.; Danarti, R.; Hertiani, T. Micro-titer plate assay for measurement of total phenolic and total flavonoid contents in medicinal plant extracts. *Arab. J. Chem.* **2023**, *16*, 105003. [CrossRef]
33. Lichtenthaler, H.K. Chlorophylls and carotenoids: Pigments of photosynthetic biomembranes. *Methods Enzymol.* **1987**, *148*, 350–382.
34. Rajalakshmi, K.; Banu, N. Extraction and Estimation of Chlorophyll from Medicinal Plants. *Int. J. Sci. Res.* **2015**, *4*, 209–212.
35. Zhou, Z.L.; Wang, G.-Y.; Wang, X.L.; Huang, X.J.; Zhu, Z.S.C.; Wang, L.L.; Yang, Y.P.; Duan, Y.W. Flower color polymorphism of a wild Iris on the Qinghai-Tibet plateau. *BMC Plant Biol.* **2023**, *23*, 633. [CrossRef]
36. Li, Z.M.; Zhou, H.G.; Chen, Y.; Chen, M.Y.; Yao, Y.T.; Luo, H.H.; Wu, Q.; Wang, F.L.; Zhou, Y.W. Analysis of Transcriptional and Metabolic Differences in the Petal Color Change Response to High-Temperature Stress in Various Chrysanthemum Genotypes. *Agronomy* **2024**, *14*, 2863. [CrossRef]
37. Wu, D.; Zhuang, F.C.; Wang, J.R.; Gao, R.Q.; Zhang, Q.N.; Wang, X.L.; Zhang, G.C.; Fang, M.H.; Zhang, Y.L.; Li, Y.H.; et al. Metabolomics and Transcriptomics Revealed a Comprehensive Understanding of the Biochemical and Genetic Mechanisms Underlying the Color Variations in Chrysanthemums. *Metabolites* **2023**, *13*, 742. [CrossRef]
38. Shi, Q.Q.; Li, L.; Zhou, L.; Wang, Y. Morphological and Biochemical Studies of the Yellow and Purple–red Petal Pigmentation in *Paeonia delavayi*. *HortScience* **2018**, *53*, 1102–1108. [CrossRef]
39. Hua, M.; Yuan, X.L.; Yang, W.; Chen, J.; Hu, Y.L.; Bing, T.; Yang, Y.M.; Juan, W. Analysis of Anthocyanins and Flavonols in six Different Colors of Petals of *Paeonia delavayi* by High Performance Liquid Chromatography. *J. West China For. Sci.* **2017**, *46*, 40–45. (In Chinese) [CrossRef]
40. Miyagawa, N.; Miyahara, T.; Okamoto, M.; Hirose, Y.; Sakaguchi, K.; Hatano, S.; Ozeki, Y. Dihydroflavonol 4-reductase activity is associated with the intensity of flower colors in delphinium. *Plant Biotechnol.* **2015**, *32*, 249–255. [CrossRef]
41. Stevens, J.T.E.; Wheeler, L.C.; Williams, N.H.; Norton, A.M.; Wessinger, C.A. Predictive Links between Petal Color and Pigment Quantities in Natural *Penstemon* Hybrids. *Integr. Comp. Biol.* **2023**, *63*, 1340–1351. [CrossRef]
42. Wan, W.Y.; Jia, F.F.; Liu, Z.Y.; Sun, W.; Zhang, X.F.; Su, J.S.; Guan, Z.Y.; Chen, F.D.; Zhang, F.; Fang, W.M. Quantitative evaluation and genome-wide association studies of chrysanthemum flower color. *Sci. Hortic.* **2024**, *338*, 113561. [CrossRef]
43. Zhang, Y.; Xu, Y.C.; Zhang, X.X.; Xue, J.Q.; Zhang, Q. Investigation and study of the population and ecological environment of *P. delavayi*. *Jiangsu Agric. Sci.* **2009**, 415–417. (In Chinese)
44. Grossenbacher, D.L.; Lo, M.S.; Waddington, M.E.; O'Dell, R.; Kay, K.M. Soil and climate contribute to maintenance of a flower color polymorphism. *Am. J. Bot.* **2025**, *113*, e70018. [CrossRef] [PubMed]
45. Sullivan, C.; Koski, M. The effects of climate change on floral anthocyanin polymorphisms. *Proc. R. Soc. B Biol. Sci.* **2021**, *288*, 20202693. [CrossRef]
46. Li, K. Research on Conservation Biology and Genetic Diversity of Paeonia delavayi Complex (Peaoniaceae). Ph.D. Thesis, Chinese Academy of Forestry, Beijing, China, 2013.
47. Landi, M.; Tattini, M.; Gould, K.S. Multiple functional roles of anthocyanins in plant-environment interactions. *Environ. Exp. Bot.* **2015**, *119*, 4–17. [CrossRef]
48. Winkel-Shirley, B. Flavonoid Biosynthesis. A Colorful Model for Genetics, Biochemistry, Cell Biology, and Biotechnology. *Plant Physiol.* **2001**, *126*, 485–493. [CrossRef] [PubMed]

49. Clifford, M.N. Anthocyanins—Nature, occurrence and dietary burden. *J. Sci. Food Agric.* **2000**, *80*, 1063–1072. [CrossRef]
50. Volkova, P.A.; Schanzer, I.A.; Meschersky, I.V. Colour polymorphism in common primrose (*Primula vulgaris* Huds.): Many colours–many species? *Plant Syst. Evol.* **2013**, *299*, 1075–1087. [CrossRef]

Disclaimer/Publisher's Note: The statements, opinions and data contained in all publications are solely those of the individual author(s) and contributor(s) and not of MDPI and/or the editor(s). MDPI and/or the editor(s) disclaim responsibility for any injury to people or property resulting from any ideas, methods, instructions or products referred to in the content.